

On the Use of Regulator Theory in Neuroscience with Implications for Robotics

Mireille E. Broucke

Electrical and Computer Engineering, University of Toronto, Toronto, Canada

Keywords: Regulator Theory, Adaptive Internal Models, Motor Control, Cerebellum.

Abstract: We survey recent results on the use of regulator theory in neuroscience, particularly to model the contribution of the cerebellum to motor systems. Based on our study of the slow eye movement systems as well as visuomotor adaptation, several themes emerge, including a promising structural model of the cerebellum, and insights on how the cerebellum may enable and disable internal models. Implications for robotics are discussed at the end of the paper.

1 INTRODUCTION

This paper presents an overview of our recent work on applying regulator theory to problems of neuroscience, particularly modeling the contribution of the cerebellum to human motor systems. We present a structural model that is inspired by the cerebellar anatomy. This model will be recognizable as an adaptive observer. Our working hypothesis is that the primary function of the cerebellum is *disturbance rejection* of exogenous reference and disturbance signals. This interpretation of cerebellar function places the *internal model principle* at front and center (Francis and Wonham, 1976). The idea to interpret the cerebellum in terms of disturbance rejection is not new. For instance, the first proposal by Stephen Lisberger on the role of internal models in the cerebellum in his survey paper (Lisberger, 2009) is consistent with a role of disturbance rejection. Lisberger describes internal models as providing “a model of the inertia of real-world objects in motion”; see also (Cerminara et al., 2009). What is new is our use of regulator theory to mathematically model the cerebellum.

This paper is informal. We suppress mathematical details as much as we can, without necessarily compromising on completeness. We want to draw connections between different areas that are typically not compared side by side: for instance, regulator designs for disturbance rejection with a systems-level model of the cerebellum; specific models of motor systems compared with each other; even comparisons between continuous-time and discrete-time processes both associated with the cerebellum. In making this sur-

vey, several themes or takeaways emerge, which we already summarize here for the reader who is interested in the main points (meanings of specific terms are found in the main text below):

- The cerebellar architecture resembles that of an adaptive observer (Kreisselmeier, 1977; Kanelakopoulos and Kokotovic, 1995).
- The *nucleo-cortical pathway* is in direct correspondence with the internal model principle in the sense that without this pathway, the internal model principle would not be satisfied by the mathematical model.
- The theory suggests that the *granular layer filters* of the cerebellum must synchronize on the same time constants for filtering *mossy fiber* (MF) inputs to the same cerebellar modules.
- Mathematically speaking, there is considerable flexibility in terms of how MF inputs to the cerebellum may be combined or “pre-bundled”.
- The mathematical models suggest that some MF inputs have the role to ensure that they are not cancelled out by the cerebellum. This seemingly contradictory role may potentially lead to misinterpretations of the function of certain cerebellar modules. On the other hand, the collaborative role between the cerebellum and feedforward signals is well known.
- The cerebellum may well be the unique brain structure that is wired to handle the dangerous operation of shutting on and off internal models for satisfaction of the internal model principle.
- Research on the cerebellum has implications for robotics.

2 CEREBELLUM

The locus of internal models in the brain is believed to be the *cerebellum*. The cerebellum is a major brain region positioned at the back of the head, partly covered by the *cerebral cortex*, and itself covering the *brainstem*. In 1967 nobel prize winner John Eccles and his co-authors laid out the *microcircuit* of the cerebellum (Eccles et al., 1967). Their work showed that the cerebellum contains relatively few neuron types, and that it has a laminated structure with a repeating architectural pattern pervading each layer or functional *module*. Each module has only two input pathways and a single output pathway (Apps et al., 2018).

The first of two input pathways to the cerebellum is via the *mossy fiber* (MF) inputs. The MFs carry a rich flow of information from sensory inputs as well as the output of the cerebellum itself. Mossy fiber outputs are received by tens of billions of *granule cells*, the most common cell type of the brain. The axons of the granule cells form *parallel fibers*, which connect with the dendrites of the principal neuron type of the cerebellum, the *Purkinje cells* (PCs). Each PC receives synaptic connections from as many as 200,000 parallel fibers, resulting in a massive fan-in of information. The second input pathway to the cerebellum is via the *climbing fibers*, which are the axons of cells from part of the brainstem called the *inferior olive*. The climbing fiber input carries a sensory error signal, and each climbing fiber forms a powerful connection with a single PC. Climbing fibers are capable to modify the strength of the synapse between parallel fiber inputs onto the PCs. The PC axons project to the *deep cerebellar nuclei* and the *vestibular nuclei*, forming the only output pathway from the cerebellum.

Notable features of the anatomical structure from a control perspective are:

- (i) The cerebellum has a purely feedforward structure. Information flows from the MF inputs to granule cells and then via the parallel fibers to the PCs. The PCs send their outputs to the deep cerebellar nuclei and vestibular nuclei.
- (ii) Each functional module of the cerebellum is identical to the others and performs the same neural computation. The only distinction between modules is in terms of the input and output connections to other regions of the brain.
- (iii) Each functional module of the cerebellum processes its own sensory error signal received via the climbing fiber inputs from a circumscribed region of the inferior olive. Each module sends its output to a circumscribed region in the cerebellar nuclei or vestibular nuclei.
- (iv) The adaptive capability of the cerebellum is provided by the climbing fiber input which changes the strength of the synapse between the parallel fibers and the PCs.
- (v) Mossy fibers projecting to a similar region of the cerebellar cortex encode similar information.
- (vi) Each of the deep cerebellar nuclei and the vestibular nuclei has a projection to the MF inputs of the cerebellum. This projection is termed the *nucleo-cortical pathway* and is regarded to provide an *efferece copy* of the motor command issued by the cerebellum (Ruigrok, 2011; Houck and Person, 2014).

3 STRUCTURAL MODEL

The features we have highlighted suggest a *structural model* associated with a single cerebellar module. This model that does not reveal function but accords with cerebellar structure at a systems level:

$$\dot{x} = Ax + Bu + Ed_1 \quad (3.1a)$$

$$e = Cx + Dd_2 \quad (3.1b)$$

$$\dot{w}_1 = F_1 w_1 + G_1 u_{mf,1} \quad (3.1c)$$

$$\vdots$$

$$\dot{w}_k = F_k w_k + G_k u_{mf,k} \quad (3.1d)$$

$$\dot{w}_{k+1} = F_{k+1} w_{k+1} + G_{k+1} u_{im} \quad (3.1e)$$

$$\hat{w} = (w_1, \dots, w_{k+1}) \quad (3.1f)$$

$$\hat{\psi} = \gamma e \hat{w}^T \quad (3.1g)$$

$$u_{im} = \hat{\psi} \hat{w} \quad (3.1h)$$

$$u = u_s + u_{im} \quad (3.1i)$$

Equation (3.1a) represents the open-loop system under regulation by the cerebellum: *horizontal eye position, eye velocity, hand position, hand grip force, gait, stance*, and so forth. Signal $e \in \mathbb{R}$ is an error that the cerebellum is tasked with asymptotically driving to zero. Signal $d_1 \in \mathbb{R}$ is a persistent exogenous disturbance entering at the plant input. Signal $d_2 \in \mathbb{R}$ is a persistent exogenous disturbance entering at the error measurement. Distinct MF input signals are $u_{mf,1}, \dots, u_{mf,k}, u_{im} \in \mathbb{R}$, which arrive by way of the filters (3.1c)-(3.1e) with corresponding filter states w_1, \dots, w_{k+1} . We assume each F_i , $i = 1, \dots, k+1$ is Hurwitz. These filters are in analogy with the lead-lag filters utilized in (Fujita, 1982) to model the granular layer, but we allow a more general interpretation here. The filter (3.1e) is particularly important as it models the nucleo-cortical pathway. The equation (3.1g) is the standard least-mean-squares (LMS) parameter adaptation law to model the modifiable synapses between parallel fibers and PCs. The signal e in (3.1g) is

supplied by the climbing fiber input. Parameter $\gamma > 0$ is the adaptation rate. The output of the cerebellum is u_{im} , and the motor command is u , which includes u_s for closed-loop stability, if needed. A control theorist will recognize the structural model to be an *adaptive observer* (Kreisselmeier, 1977; Kanellakopoulos and Kokotovic, 1995).

4 DISTURBANCE REJECTION

The structural model does not endow the cerebellum with any particular function except that of filtering MF inputs with parameter adaptation. Our working hypothesis is that the primary function of the cerebellum is *disturbance rejection*, bringing into view *regulator theory* (Wonham, 1985). In this section we look at a representative *regulator design* to solve the disturbance rejection problem so that we can bring out comparisons with the structural model. The design utilizes *adaptive internal models* (Nikiforov, 2004a; Nikiforov, 2004b).

Consider the open-loop system

$$\dot{x} = Ax + B(u + d) \quad (4.1a)$$

$$\dot{w} = Fw + Gd \quad (4.1b)$$

$$d = \psi w \quad (4.1c)$$

$$e = Cx, \quad (4.1d)$$

where $x \in \mathbb{R}^n$ is the *state*, $w \in \mathbb{R}^q$ is the *exosystem state*, $u \in \mathbb{R}$ is the *control input*, $e \in \mathbb{R}$ is the *error* to be regulated, and $d \in \mathbb{R}$ is a persistent, exogenous *disturbance* signal entering the plant at the control input. The *exosystem* (4.1b) provides a model of the frequency content of the disturbance in terms of a row vector of unknown parameters $\psi \in \mathbb{R}^{1 \times q}$.

Problem 4.1 (Regulator Problem). Consider the system (4.1). Find a *error feedback regulator*

$$\dot{x}_c = Fx_c + Ge \quad (4.2a)$$

$$u = Hx_c + Ke, \quad (4.2b)$$

with *regulator state* $x_c(t) \in \mathbb{R}^p$, such that the following conditions are met:

(AS) The equilibrium $(0, 0) \in \mathbb{R}^n \times \mathbb{R}^p$ of the *unforced closed-loop system*

$$\dot{x} = (A + BKC)x + BHx_c \quad (4.3a)$$

$$\dot{x}_c = Fx_c + GCx \quad (4.3b)$$

is asymptotically stable.

(R) The forced closed-loop system satisfies: for all initial conditions $(x(0), x_c(0), w(0))$, $e(t) \rightarrow 0$. \triangleleft

The following assumptions are standard in the regulator theory literature; see (Saberi et al., 2000) for more background: (A1) (A, B) is controllable. (A2) (C, A) is observable. (A3) $S := F + G\psi$ has simple eigenvalues on the imaginary axis. (A4) $\det \begin{bmatrix} A - \lambda I & B \\ C & 0 \end{bmatrix} \neq 0$ for all $\lambda \in \sigma(S)$. (A5) (F, G) is controllable, F is Hurwitz, and (ψ, S) is w.l.o.g. an observable pair. (A6) An upper bound on q is known, but the parameters of (ψ, S) are unknown. (A7) The parameters (A, B, C) are known. (A8) The measurement is x .

Consider a control input of the form (3.1i). The first component u_s is selected for stabilization: choose $u_s = Kx$ such that $(A + BK)$ is Hurwitz. The second component u_{im} is designed to satisfy the *internal model principle* (Francis and Wonham, 1976). Consider an *adaptive internal model* from (Nikiforov, 2004a):

$$\dot{w}_0 = Fw_0 + FNx \quad (4.4a)$$

$$\dot{w}_1 = Fw_1 - NAx \quad (4.4b)$$

$$\dot{w}_2 = Fw_2 - NBu \quad (4.4c)$$

$$\dot{\hat{w}} = w_0 + Nx + w_1 + w_2 \quad (4.4d)$$

$$\dot{\hat{\psi}} = \gamma(B^T Px)\hat{w}^T \quad (4.4e)$$

$$u_{im} = -\hat{\psi}\hat{w}, \quad (4.4f)$$

where N satisfies $NB = G$, $\hat{\psi}$ is an estimate of ψ , $\gamma > 0$ is the adaptation rate, and $P \in \mathbb{R}^{n \times n}$ is the symmetric, positive definite solution of the Lyapunov equation $(A + BK)^T P + P(A + BK) = -Q$, with $Q \in \mathbb{R}^{n \times n}$ symmetric and positive definite.

Now we observe

$$\begin{aligned} \dot{\hat{w}} &= Fw_0 + FNx + N(Ax + Bu + Bd) \\ &+ Fw_1 - NAx + Fw_2 - NBu \\ &= F\hat{w} + Gd. \end{aligned} \quad (4.5)$$

Thus, \hat{w} evolves according to the same dynamics as in (4.1b). Define the *estimation error* $\tilde{w} = w - \hat{w}$. Then $\dot{\tilde{w}} = F\tilde{w}$, and since F is Hurwitz, $\tilde{w}(t) \rightarrow 0$, so \hat{w} provides an estimate of the exosystem state w . Further, (4.4) satisfies the internal model principle by way of (4.4c). For suppose that $\hat{\psi} = \psi$. Substituting u into (4.4c), we have

$$\begin{aligned} \dot{w}_2 &= Fw_2 - NB(u_s + u_{im}) \\ &= (F + G\psi)w_2 + G\eta_2, \end{aligned}$$

where $\eta_2 = \psi(w_0 + Nx + w_1) - u_s$. As such, this filter includes the unstable poles of the exosystem. Finally, the following result is proved in (Battle and Broucke, 2021).

Theorem 4.1. Consider the system (4.1) satisfying Assumptions (A1)-(A8), and the regulator (4.4). Suppose $A + BK$ is Hurwitz. Then this regulator solves the disturbance rejection problem.

In comparing (4.4) with (3.1), there are three important points:

- (i) The filter (4.4c), which fulfills the requirements of the internal model principle, corresponds to the nucleo-cortical pathway in (3.1e).
- (ii) The model (4.4) bundles together filter inputs Nx , Ax , and Bu in (4.4a)-(4.4c) based on prior knowledge of the plant parameters. However, these filter inputs need not be aggregated in this way. Mathematically speaking, states or other sensory inputs may arrive as filter inputs according to a number of patterns or combinations, potentially depending on the structure of the open-loop system. This mathematical flexibility, in turn, may imply that an “unpacking” of MF inputs to the cerebellum is necessary to determine their constituent components, making the modeling problem more challenging.
- (iii) The model (4.4) requires that all the filters (4.4a)-(4.4c) have synchronized to utilize the same filter time constants, i.e. $F_i = F_j$. Since the filters (3.1c)-(3.1e) or (4.4a)-(4.4c) are nominally intended to model the granular layer of the cerebellum, this raises the question of whether the granular layer is capable of some form of dynamic synchronization.

While we have identified intriguing analogies between cerebellar structure and internal model designs for disturbance rejection from regulator theory, the comparison is still somewhat superficial. The *oculomotor system*, discussed in the next section, provides more concrete evidence that such analogies can be fruitful toward model building.

5 OCULOMOTOR SYSTEM

The *oculomotor system* comprises several eye movement systems: the *vestibulo-ocular reflex* (VOR), *optokinetic system* (OKS), the *gaze fixation system*, the *smooth pursuit system*, the *vergence system*, and the *saccadic system*. The oculomotor system provides a good starting point for studying the cerebellum because it has a very simple plant (the eyeball), and it is believed to provide the blueprint for all other motor systems (Leigh and Zee, 2015).

5.1 VOR, Smooth Pursuit, and Gaze Holding

In (Broucke, 2020; Broucke, 2021) we presented a model of the VOR, smooth pursuit, and gaze holding

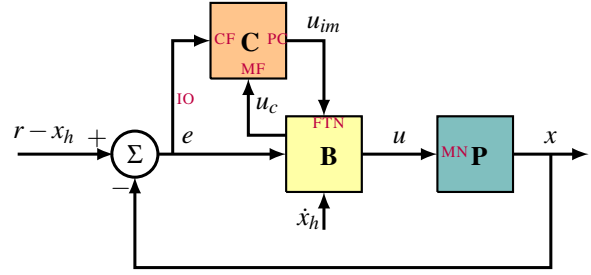


Figure 1: Control architecture for the VOR, gazing holding, and smooth pursuit systems.

for horizontal motion of one eye by applying an adaptive internal model design from (Serrani and Isidori, 2000; Serrani et al., 2001). Let $x \in \mathbb{R}$ be the horizontal eye angle, x_h the horizontal head angle, and r the horizontal angular position of a target. The model is:

$$\dot{x} = -K_x x + u \quad (5.1a)$$

$$e = r - x - x_h \quad (5.1b)$$

$$\dot{\hat{x}} = -K_x \hat{x} + u \quad (5.1c)$$

$$\dot{w}_1 = F w_1 + G u_s \quad (5.1d)$$

$$\dot{w}_2 = F w_2 + G u_{im} \quad (5.1e)$$

$$\hat{w} := w_1 + w_2 \quad (5.1f)$$

$$\dot{\hat{\psi}} = \gamma e \hat{w}^T \quad (5.1g)$$

$$u_b = \alpha_x \hat{x} - \alpha_{VOR} \dot{x}_h \quad (5.1h)$$

$$u_s = K_e e \quad (5.1i)$$

$$u_{im} = \hat{\psi} \hat{w} \quad (5.1j)$$

$$u = u_b + u_s + u_{im} \quad (5.1k)$$

Equation (5.1a) is the first order model of the oculomotor plant (Sylvestre and Cullen, 1999). Equation (5.1b) is the *retinal error*, the difference between the target angle r and the gaze angle $x + x_h$. It is this error that the cerebellum is tasked with driving asymptotically to zero. Equation (5.1c) models the brainstem *neural integrator* (Robinson, 1974) which acts as an observer to provide an estimate \hat{x} of eye position. Equations (5.1d)-(5.1g) comprise the adaptive internal model in the cerebellum. The motor command u has a component u_b corresponding to a brainstem-only pathway for pure feedforward signals, a component $u_s = K_e e$ to improve closed-loop stability, and u_{im} , the cerebellar output from the PCs.

The model can be compared to the known neural circuit associated with these eye movement systems (Büttner and Büttner-Ennever, 2006), visualized by a block diagram in Figure 1. The error signal (5.1b) is transmitted from the *visual cortex* to the *inferior olive* (IO), where it is relayed to appropriate climbing fiber inputs (CFs) of the cerebellum (C), specifically, the module called the *floccular complex*. This is the signal e appearing in (5.1g). The cerebellum also re-

ceives MF inputs from the *medial vestibular nuclei* (MVN) in the brainstem (B). These are the MF inputs in (5.1d)-(5.1d). The sole output of the cerebellum is u_{im} , transmitted via its PCs to *floccular target neurons* (FTNs) in the MVN (Ramachandran and Lisberger, 2008). The MVN also receives a head velocity signal from the semicircular canals of the ear, signal \dot{x}_h in (5.1h), corresponding to the VOR. The parameter α_{vor} is the *VOR gain*. The eye position signal $\alpha_x \hat{x}$ corresponds to the projection from the brainstem *nucleus prepositus hypoglossi* (NPH) to the MNs. The output of the MVN is sent both to the neural integrator (NI) in the NPH and directly to the *oculomotor neurons* (MNs) of the oculomotor plant (P).

As we discussed above, the MF inputs in (5.1d)-(5.1e) may be bundled in a number of ways with no effect on the overall behavior. For example, the two filters could be combined into one, as was done in (Serrani and Isidori, 2000), for a more parsimonious model

$$\dot{\hat{w}} = F\hat{w} + G(u_s + u_{im}).$$

This modification affects the choice of parameters being adapted, but it does not affect overall model behavior. Alternatively one could write

$$\begin{aligned} \dot{w}_1 &= Fw_1 + FG e \\ \dot{w}_2 &= Fw_2 + G(u - u_b) \\ \hat{w} &:= (w_1, w_2) \end{aligned}$$

The feedforward signals in u_b are now arriving as MF inputs to be subtracted from the overall motor command. This subtraction of feedforward signals is required so that their effect is not cancelled by the cerebellum (the cerebellum provides a top-up to the action of feedforward signals). Depending on the origin of the constituent components of the motor command u in the brain, such an explicit subtraction of certain MF inputs may arise, if not for the floccular complex, possibly in another cerebellar module. Such a situation would certainly cloud an understanding of the role of certain MF inputs to the cerebellum.

The model (5.1) recovers the standard lesion, behavioral, and neurological experiments associated with the VOR, gaze holding, and smooth pursuit; see (Broucke, 2020; Broucke, 2021). Here we discuss two interesting experiments which highlight the special capabilities of the cerebellum.

A first experiment called the *error clamp* explores the role of the error signal using a technique called *retinal stabilization* (Barnes et al., 1995; Morris and Lisberger, 1987; Stone and Lisberger, 1990). A monkey is trained to track a visual target moving horizontally at constant speed. After reaching steady-state, the error is optically clamped at zero using an experimental apparatus that centers the target image

directly on the fovea. In experiments it is observed that, despite zero error, the eye continues to track the target for some time after. Neuroscientists postulate so called *extraretinal signals* drive the smooth pursuit system. Figure 2 depicts the error clamp with our model, showing on the left that the eye continues to track the target despite the measurement being clamped at $e \equiv 0$ during the time interval $t \in [5, 6]$. The right figure shows the (physical) error, showing that tracking is not robust during the time interval that the measurement is clamped. In the second experiment called *target blanking*, a horizontally moving target is temporarily occluded, yet the eye continues to track the target (Cerminara et al., 2009; Churchland et al., 2003); researchers have postulated the brain has an internal model of the motion of the target. Indeed, direct measurement of the appropriate PCs of the cerebellum shows that they remain active during the time that the target is occluded.

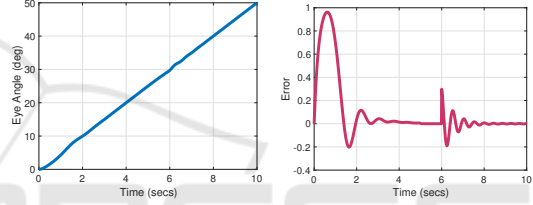


Figure 2: Smooth pursuit with an error clamp during $t \in [5, 6]$ s. The eye angle x on the left and the error e on the right.

Let's consider the meaning of these experiments in terms of (5.1). In the first experiment, the error is clamped at zero, so we can set $e \equiv 0$ to obtain

$$\begin{aligned} \dot{w}_1 &= Fw_1 \\ \dot{w}_2 &= Fw_2 + Gu_{im} \\ \hat{w} &:= w_1 + w_2. \end{aligned}$$

Since F is Hurwitz, the first filter state w_1 in steady-state is zero. Then the second filter evolves according to $\dot{w}_2 = (F + G\psi)w_2$, where $F + G\psi$ is marginally stable by (A3) (and assuming parameters have converged). Clearly w_2 provides the drive for continued pursuit during the error clamp, and it depends on the nucleo-cortical pathway. However, in the second experiment there is no error signal while the target is occluded. It would certainly be paradoxical for the cerebellum to continue to supply (on its own) a drive for pursuit when there is no sensory error. We postulate that a higher brain center gates the activity of the nucleo-cortical pathway. When there is no error signal and/or the subject is not interested in an external stimulus, then the pathway is disabled in order to

arrive at the stable model

$$\begin{aligned}\dot{w}_1 &= Fw_1 \\ \dot{w}_2 &= Fw_2 \\ \hat{w} &:= w_1 + w_2,\end{aligned}$$

in which all filter states gradually decay to a quiescent level of activity. However, when the error signal is temporarily dropped but the subject remains interested in the stimulus (e.g. a lion pursuing prey), then the nucleo-cortical pathway is not disabled. Finally, these experiments raise intriguing questions for regulator theory. Are there engineering contexts when a regulator should be capable to distinguish no error measurement from a zero error measurement?

5.2 Optokinetic System

In the previous section we considered a model of a part of the cerebellum, the floccular complex (FC), involved in regulation of the vestibulo-ocular reflex, smooth pursuit, and gazing hold eye movement systems. This section discusses a second functional module of the cerebellum, the nodulus-uvula (NU) which is responsible for regulating *the optokinetic system*.

The optokinetic system is an eye movement system to stabilize vision on a full-field moving visual surround. This eye movement system contrasts with the eye movement systems of the previous section whose goal is to stabilize an object on the fovea. How the optokinetic system interacts with the other eye movement systems is of great interest scientifically, but also theoretically from the perspective of control theory: can parallel adaptive internal models work collaboratively to regulate the same error? Or does the brain utilize a switching mechanism to switch from one adaptive internal model to the other, reminiscent of switched system architectures for adaptive control (Narendra and Annaswamy, 1989)?

Pioneering experimental work in the 1970's on the optokinetic system (Cohen et al., 1977; Raphan et al., 1979; Waespe and Henn, 1978a; Waespe and Henn, 1978b) lead to the discovery of the velocity storage mechanism (VSM), a behavior in which eye velocity is stored while following a constant velocity visual surround, even with intervening *saccades* (a fast reset of eye position) in a behavior called *nystagmus*. A striking feature of the VSM is that it partially meets the requirements of the internal model principle, as if evolution made a first attempt at architecting a neural internal model.

In (Battle and Broucke, 2021) we proposed a

model of the optokinetic system given by

$$\dot{x}_1 = x_2 \quad (5.2a)$$

$$\dot{x}_2 = \alpha_2(-x_2 - K_x x_1 + u) \quad (5.2b)$$

$$e = \dot{x}_w - \dot{x}_h - x_2 \quad (5.2c)$$

$$\dot{\hat{x}} = -K_x \hat{x} + u \quad (5.2d)$$

$$\dot{v} = -K_v v + K_v e \quad (5.2e)$$

$$\dot{w}_0 = Fw_0 + FGe \quad (5.2f)$$

$$\dot{w}_1 = Fw_1 - Ge \quad (5.2g)$$

$$\dot{w}_2 = Fw_2 - Gu_{im} \quad (5.2h)$$

$$\dot{w}_3 = Fw_3 - G\hat{x} \quad (5.2i)$$

$$\dot{w}_4 = Fw_4 - G\dot{x}_h \quad (5.2j)$$

$$\dot{w}_5 = Fw_5 - Gv \quad (5.2k)$$

$$\hat{w} = (w_0 + Ge, w_1, w_2, w_3, w_4, w_5) \quad (5.2l)$$

$$\dot{\hat{w}} = \gamma e \hat{w}^T \quad (5.2m)$$

$$u_{im} = \hat{\psi} \hat{w} \quad (5.2n)$$

$$u_b = \alpha_x \hat{x} - \alpha_{vor} \dot{x}_h + \alpha_{ok} e + \alpha_v v \quad (5.2o)$$

$$u = u_b + u_{im}. \quad (5.2p)$$

We utilized a second-order model of the oculomotor plant in (5.2a)-(5.2b), with x_1 the horizontal eye angle and x_2 the eye angular velocity, because the optokinetic system stabilizes eye velocity, not eye position. The error signal e in (5.2c) to be regulated by the cerebellum is the *retinal slip velocity*, the difference between the horizontal angular velocity of the visual field \dot{x}_w and the gaze velocity $x_2 + \dot{x}_h$. A non-zero \dot{x}_w is induced in experiments when a subject is seated inside a rotating optical drum. The brainstem neural integrator again appears in (5.2d). Equation (5.2e) is the *velocity storage integrator* of the optokinetic system (Cohen et al., 1977). The motor command u is now regarded as an acceleration input; v is the state of the velocity storage integrator; $\alpha_{ok} e$ captures the drive provided by the *optokinetic reflex*, where α_{ok} is the called the *optokinetic gain*; the vestibulo-ocular reflex is modeled by $\alpha_{vor} \dot{x}_h$, as before. The term $\alpha_v v$ captures the drive provided by the velocity storage integrator. Finally, we mention that there is no stabilizing feedback u_s in this model because the velocity dynamics of the oculomotor plant are already highly stable.

In comparing this model to the structural model (3.1), we observe the additional filters (5.2f)-(5.2k) driven by feedforward signals \hat{x} , \dot{x}_h , and v . Mathematically speaking, it can be shown that if these signals are not included as MF inputs, then they would be cancelled or rejected by the activity of the nodulus/uvula as predicted by the model. Thus, a pattern we have already highlighted on the variable roles of certain MF inputs is reinforced again with this model: mathematically speaking, MF inputs may either ap-

pear because they are directly involved in disturbance estimation or they appear to avoid being cancelled by the cerebellum.

The model (5.2) is consistent with the neural circuit, and it recovers five standard behaviors of the optokinetic system: optokinetic nystagmus (OKN); optokinetic after-nystagmus (OKAN I); OKAN suppression; OKN suppression; and OKAN II. For instance, OKN is an eye movement in which the eye tracks the velocity of a (full-field) moving visual surround during the so-called *slow phase*, followed by a saccade to rapidly reset the eye position to zero in the *fast phase* (Cohen et al., 1977; Raphan et al., 1979). OKAN I is a behavior following OKN when the lights are turned off. During OKAN I nystagmus continues in the same direction as OKN, even though there is no visual stimulation (Cohen et al., 1977; Büttner et al., 1976).

Figure 3 shows simulation results for OKN and OKAN I using our model, with the optokinetic drum rotating at a constant velocity of 60 deg/s for 60s. The initial jump in slow phase eye velocity is attributable to the large retinal slip velocity at the onset of the experiment and the charging of the VSM. The non-zero steady-state error during OKN is observed because the NU internal model is “untrained”. Once the lights are extinguished at $t = 60$ s, visual signals are no longer present and the cerebellum is effectively inactive, the signal e is unavailable, and $u_{im} = 0$ (based on gating the nucleo-cortical pathway). This causes the slow-phase eye velocity to rely on the dynamics from the VSM, which slowly dissipates its stored velocity, creating OKAN I.

If the subject is involved in repeated trials of the same experiment eliciting OKN and OKAN I, the NU internal model is “trained” over time. Consequently, the OKN steady-state slow-phase eye velocity increases (Miki et al., 2020, Fig 1); the OKAN I time constant decreases (Cohen et al., 1977, Fig 7); and the OKAN I duration decreases (Waespe and Henn, 1978b, Fig 2, 3). These results are shown on the right of Figure 3.

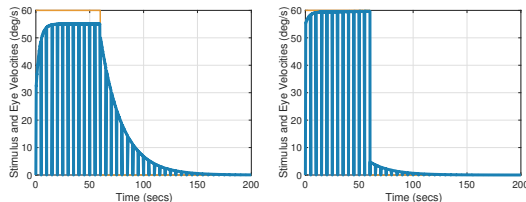


Figure 3: Untrained (left) and trained (right) OKN and OKAN I.

This section has demonstrated that a disturbance rejection interpretation of cerebellar function can be propitious to arrive at plausible models for one motor system: the oculomotor system. However, one

may also utilize regulator theory to understand other adaptive behaviors that are best modeled as discrete, repetitive processes. Perhaps the most widely studied adaptive, discrete process is visuomotor adaptation, considered in the next section.

6 VISUOMOTOR ADAPTATION

Visuomotor adaptation is a subconscious, “machine-like” brain process taking place over repetitive trials and elicited by a *visual error* closely following the execution of a movement. Visuomotor adaptation is intended to calibrate over a lifetime the mapping between what is seen and how to move. As a means to expose the underlying computations of this brain process, neuroscientists create experiments that artificially perturb what is seen by the subject during movement. Examples include saccades with an intersaccadic step of the target (Kojima et al., 2004); the *visuomotor rotation experiment* with fast arm reaches (Smith et al., 2006; Shadmehr and Wise, 2005); and throwing darts while looking through prism glasses (Martin et al., 1996).

Visuomotor adaptation experiments consist of repetitive trials of a certain movement such as a saccade or arm reach. The trials are classified by type, and sequences of blocks of trials of specific types are utilized to elicit so-called dynamic behaviors of adaptation. A *baseline* (B) block familiarizes the subject with the experimental apparatus under unperturbed, normal conditions. A *learning* (L) block occurs after a baseline block when a perturbation or disturbance is introduced. A *washout* (W) block follows a learning block when the perturbation is removed. An *unlearning* (U) block follows a learning block when the perturbation changes in sign but not magnitude relative to the learning block. A *relearning* (R) block is a second learning block with the same perturbation. A *down-scaling block* (D) is a second learning block in which the perturbation is set to a fraction of its value in the first learning block. A *no-visual-feedback* (N) block is a block of trials in which no error measurement is presented to the subject. An *error clamp* (C) block is a block of trials when the error measurement presented to the subject is clamped artificially to a value unrelated to the subject’s movements. When blocks of trials are sequenced in a particular order and with a particular number of trials in each block, then several phenomena emerge in experiments:

- *Savings* is a behavior in which learning is sped up in the second learning block relative to the first one.

- *Reduced savings* is a behavior in which savings is reduced by inserting a washout block of trials after the unlearning block. After the washout block, relearning does not proceed as rapidly as in the savings experiment.
- *Anterograde interference* is a behavior in which a previously learned task reduces the rate of subsequent learning of a different (and usually opposite) task.
- *Rapid unlearning* is a behavior in which the rate of unlearning is faster than the rate of initial learning, if the number of trials in the learning block is small.
- *Rapid downscaling* is a behavior in which the rate of learning in a secondary learning block is faster when the rotation is set to a fraction of its value in the initial learning block.
- *Spontaneous recovery* is a behavior observed during the washout block of a BLUW experiment in which the response partially “rebounds” to its value at the end of the learning block rather than converging monotonically to zero.

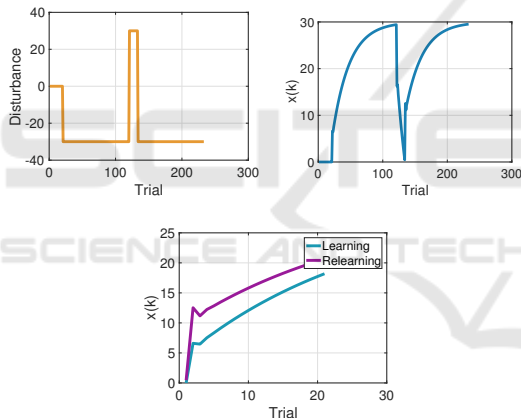


Figure 4: Savings in a BLUR experiment. In the bottom figure $x(k)$ during the learning block is plotted in blue superimposed with a horizontally shifted version of $x(k)$ during the relearning block in purple. The purple curve is larger than the blue curve corresponding to faster learning in the relearning block.

We used regulator theory to develop a model of visuomotor adaptation in (Gawad and Broucke, 2020; Hafez et al., 2021) with the goal to recover the six standard behaviors of visuomotor adaptation. The model was based on three assumptions. First, we focused on motor adaptation tasks involving one degree of freedom of movement; for instance, horizontal movement of the eye, hand angle relative to a reference angle in a horizontal plane, forward (coronal) inclination of the body relative to a vertical reference, the horizontal angle of a dart thrown by a subject, and so forth. Second, we assumed the open-loop model is

linear time-invariant. Third, we focused on constant disturbances, as currently there is a dearth of experiments with non-constant disturbances.

Let integer k be the trial number; $x(k)$ is the state of a single degree of freedom of the body at the end of the k -th trial; $d(k)$ is an additive disturbance in the measurement during the k -th trial; and $e(k)$ is the error between a measurement $y(k) = x(k) + d(k)$ observed by the subject at the end of the k -th trial and a reference $r(k)$. Our discrete-time model of visuomotor adaptation is:

$$x(k+1) = Ax(k) + Bu(k) \quad (6.1a)$$

$$e(k) = r(k) - d(k) - x(k) \quad (6.1b)$$

$$w_0(k+1) = Fw_0(k) + FG e(k) \quad (6.1c)$$

$$w_1(k+1) = Fw_1(k) - Ge(k) \quad (6.1d)$$

$$w_2(k+1) = Fw_2(k) - Gu(k) \quad (6.1e)$$

$$\hat{w}(k) = (w_0(k) + Ge(k), w_1(k), w_2(k)) \quad (6.1f)$$

$$u(k) = Ke(k) + K_w \Psi \hat{w}(k). \quad (6.1g)$$

The open-loop system model (6.1a) provides a high-level, abstract description of the quantitative change over successive trials of a single degree of freedom of the body. The term $Ax(k)$ models a retention or memory mechanism of the state in the previous trial. We assume the filters (6.1c)-(6.1e) are stable; that is, F is Schur stable. We have not written a parameter adaptation law for unknown parameters Ψ (although one may do so) since experiments show that the parameters vary extremely slowly; see (Gawad and Broucke, 2020). The controller u has the same components as before: $u_s(k) = Ke(k)$ is to improve closed-loop stability, while $u_{im} = K_w \Psi \hat{w}(k)$ is the component to satisfy the internal model principle. The parameter $0 < K_w < 1$ is explained below.

Figure 4 shows a simulation for a BLUR experiment to elicit savings. The top left figure shows the disturbance value $d(k)$ as a function of k , and the top right figure shows $x(k)$. The bottom figure shows $x(k)$ during the learning block superimposed with $x(k)$ during the relearning block. We see that relearning is faster than learning, demonstrating that savings have indeed occurred in the relearning block.

Visuomotor adaptation experiments analogous to the error clamp and target blanking experiments for the smooth pursuit system have also been performed. These provide dramatic evidence of the brain’s capability to enable or disable internal models. For instance, many experimental studies of the form BLN have been conducted on the effect of removing the visual error in an N block following a learning block (Galea et al., 2011; Kitago et al., 2013; Bond and Taylor, 2015). The major finding is that during the N block, $x(k)$ slowly returns to a nominal reference po-

sition. Further, Figure 2 of (Kitago et al., 2013) shows that the rate of decay is faster in a W block than an N block.

As we already discussed for the oculomotor system, when there is no error measurement, we must remove the signal $e(k)$ from every filter input in (6.1). To disable the internal model, it is also necessary to disable the efference copy $u(k)$ in (6.1e). The resulting internal model will consist of filters that are all stable, and therefore the response $x(k)$ will gradually return to a zero reference value. In summary, if we assume that visuomotor adaptation operates in a manner that is consistent with the oculomotor system, then gating the nucleo-cortical pathway provides an explanation for how internal models can be enabled or disabled in visuomotor adaptation. Figure 5 shows the results for (6.1) for a BLN experiment using this method to disable the internal model during the N block.

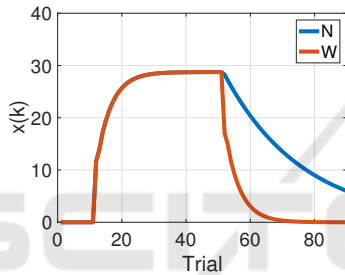


Figure 5: BLN experiment v.s. BLW experiment.

A number of error clamp experiments of the form $BLC(\mu)$ have been reported including (Smith et al., 2006; Kitago et al., 2013; Shmuelof et al., 2012; Vaswani et al., 2015). In these experiments a subject makes fast arm reaches to a target on a computer screen while observing a cursor intended to represent the hand position at the end of a reach. A disturbance $d(k)$ is introduced during the learning blocks so that the observed cursor angle is $y(k) = x(k) + d(k)$. During error clamp blocks, the error observed by the subject is clamped at a constant value $e(k) \equiv \bar{e}$. Figure 2 of (Vaswani et al., 2015) reported results with various statistics on the error clamp value. These experiments further expose interesting on/off behavior of internal models associated with visuomotor adaptation. In a $C(-2.7)$ block with $e(k) \equiv -2.7$, it is observed that the hand angle remains close to its value at end of the learning block. In a $C(0)$ block with $e(k) \equiv 0$, the hand angle returned to zero at a slow rate. Figure 6 shows the behavior of our model in a $BLC(-2.7)$ experiment. We observe the hand angle remains close to 30° , its value at the end of the learning block, as reported in (Vaswani et al., 2015). By comparison, the

right figure shows a $BLC(0)$ experiment. Now the hand angle slowly returns to zero.

The behavior in Figure 6 is nothing like what a control theorist expects of an internal model. We expect that when $e(k)$ is clamped at zero, the behavior is as in the left of the figure, but when $e(k)$ is clamped at a non-zero value, the internal model is unstable. Instead, the experiments demonstrate that the human brain has made a ‘‘hedge’’ on the internal model principle: zero error signals induce a return to a quiescent state, while a persistent, small, non-zero error is necessary to keep the internal model active. We have used the parameter $0 < K_w < 1$ to quantitatively characterize this hedge; however, this single parameter certainly does not complete the story. There are likely deeper meanings behind this curious phenomenon.

We summarize by saying that the preponderance of experimental evidence may well point to the idea that the sole reason for the special wiring of the cerebellum, particularly the nucleo-cortical pathway, is to implement the delicate operation of enabling and disabling internal models without inducing abrupt or unstable behavior in the subject.

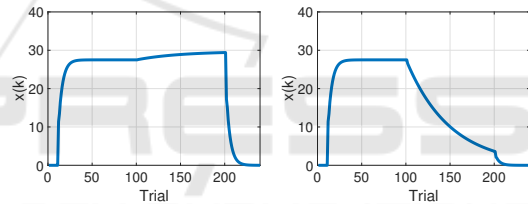


Figure 6: BLC experiment, comparing $C(-2.7)$ and $C(0)$ blocks.

7 IMPLICATIONS FOR ROBOTICS

We have given evidence that there is value to study the cerebellum from the perspective of disturbance rejection and to utilize regulator theory to derive models. We argue here that the study of the cerebellum using regulator theory has implications for robotics. We make our case using an example of a robot learning a new tool. The discussion is informal, as the primary aim is to stimulate new ideas rather than to prove correctness of fully developed algorithms, etc.

Consider a robot equipped with an arm and foveated, movable cameras resembling the functionality of the human eye. The robot is capable to perform rapid reaching movements with its arm using feedforward, pre-learned commands. The robot is tasked with performing such rapid movements while manipulating a new handheld tool - for example a brush with a long handle to remove brambles from

a dog. We pose the problem of training the robot to learn a new tool as a disturbance rejection problem. For simplicity, consider one degree of freedom of movement, say the final horizontal angle of the robot's end effector at the end of a reach. We make the following assumptions:

Assumption 7.1.

- N stationary targets are randomly positioned in the robot's visual field but sufficiently separated that the robot is able to measure a distinct error between the arm (or the tool) end effector and any foveated target. Let $r(i)$ denote the horizontal angular position of the i th target for $i = 1, \dots, N$.
- Each target i has associated to it a feedforward (non-error-based) motor command denoted $u_{f,i}$ that was acquired through prior experience during nominal behavior (without using tools). We assume $u_{f,i}$ drives the robot end-effector directly to target position $r(i)$ with negligible error under nominal conditions.
- The visual field is partitioned into sectors called *adaptation fields*. Each adaptation field has associated to it an adaptive internal model. For simplicity we assume there is only one target per adaptation field.
- The robot has the efficacy to foveate any target at the end of a reach, at will. The index of the target that is foveated at the end of the k th reach is $m(k) \in \{1, \dots, N\}$.
- The robot has the efficacy to choose any target for the next reach, at will. The index of the target for the $(k+1)$ th reach is $t(k) \in \{1, \dots, N\}$.

Let $x(k)$ represent the robot end-effector horizontal angle at the end of the k th reach, and $d(k)$ is the constant angular offset introduced by the tool. The open-loop model is:

$$\begin{aligned} x(k+1) &= u(k) \\ e(k) &= r(m(k)) - x(k) - d(k). \end{aligned}$$

The first equation says the robot is capable to move to any commanded horizontal angular position (the true nonlinear robot model may require a preliminary feedback linearization step to achieve this simple form). The second equation defines the error measured at the end of the k th reach, the angular displacement between the $m(k)$ th target and the end of the tool. Because it is highly expensive to process full-field visual information, the robot only records error measurements for targets it has foveated on. Further, we assume that the trigger signal to update any internal model is its own error signal. In other words, the robot's gaze at the end of the reach determines the internal model to be updated. The internal model update

for a target that has been foveated is:

$$\begin{aligned} w_{0,m}(k+1) &= Fw_{0,m}(k) + FG e(k) \\ w_{2,m}(k+1) &= Fw_{2,m}(k) + G(u(k) - u_{f,m}) \\ \hat{w}_m(k) &= w_{0,m}(k) + Ge(k) - w_{2,m}(k), \end{aligned}$$

where $m = m(k)$ is as above. All other internal models with $i \neq m(k)$ have an update of the form:

$$\begin{aligned} w_{0,i}(k+1) &= F_n w_{0,i}(k) \\ w_{2,i}(k+1) &= F_n w_{2,i}(k) \\ \hat{w}_i(k) &= w_{0,i}(k, i) - w_{2,i}(k) \end{aligned}$$

This second update is a proxy for "no update". We set $F_n = 0.999$, meaning the internal model i very slowly dissipates its state until the next update when $m(k) = i$. Finally the motor command is

$$u(k) = u_{f,t} + \Psi \hat{w}_t(k),$$

where $t = t(k)$ is as above, and Ψ represents unknown parameters (that have been adapted apriori, hence the adaptation process is omitted). Several observations are in order.

- We have subtracted off the feedforward command $u_{f,m}$ from the motor command $u(k)$ in analogy with our discussion for the oculomotor system. Recall that this intervention was required for the slow eye movement systems to ensure the cerebellum does not cancel the effect of useful feedforward signals. Internal models are intended to work synergistically with feedforward signals, a notion well expounded particularly with regard to the VOR (Ito, 1984).
- The internal model output that appears in the motor command is dictated by the choice of feedforward command, which is itself subject to the robot's will. That is, feedforward commands and their associated internal model output are always paired.
- Our model dissociates the updating of an internal model from the ensuing motor command. That is, some internal model updates are *unobservable*, possibly only to be revealed as *aftereffects* once the experiment is concluded.

Simulation results using this model are shown in Figure 7. There are three targets with horizontal angular positions $r(1) = 0$, $r(2) = 45$, and $r(3) = -20$. The handheld tool causes a disturbance in the arm position by an amount of -45 degrees. After a baseline block of 20 trials with no tool, the robot picks up the tool and reaches for target 1 for 60 trials, then target 2 for 60 trials, and target 3 for the last 60 trials. While the robot reaches for target 1, it glances at target 2 at the end of every 8th reach and at target 3 at the end of every 12th reach. We see in the right figure that

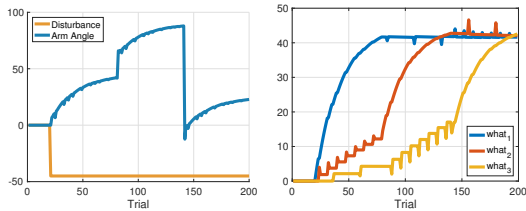


Figure 7: A robot arm reaching for each of three targets, while occasionally glancing at the other two. The left figure shows the arm angle and the right figure shows $\hat{w}_i(k)$ for the three internal models.

the internal models begin “charging up” as they collectively estimate the disturbance induced by holding the tool. By the time the robot reaches for the second target, the first internal model is almost fully charged. Only infrequent glances are needed to retain a fresh estimate of the disturbance by this internal model. Finally, by the end of the experiment, all internal models have approached a consensus value on the disturbance induced by holding a tool. The robot may save the motor memory, so if this tool is encountered again, the revised motor commands may be immediately recalled.

The model we have presented for simple tool learning was not an abstract exercise, but has been inspired by our study of visuomotor experiments with human subjects. To bring home this point, we apply our model to a well-known experiment on feed-forward (so-called explicit) strategies in visuomotor adaptation (Mazzoni and Krakauer, 2006). A subject is presented with two targets separated by a fixed angle of 45 degrees. The subject is instructed to aim for the second target at $r(2) = 45$ degrees while observing a cursor position on a computer screen displayed at the end of each reach. The cursor position has been rotated by $d(k) = -45$ degrees from the true hand angle, so that by aiming for the second target, the subject is able to make the error between the cursor and a first target at $r(1) = 0$ degrees be close to zero.

We can simulate this experiment using our learning model. We assume the subject aims for the second target in all trials, so $t(k) = 2$, according to the instructions of the experimenter. However, the subject occasionally shifts the gaze at the end of a reach to the first target (Rand and Rentsch, 2015; de Brouwer et al., 2018). Suppose the subject attends to the first target at the end of 20 percent of trials and to the second target in 80 percent of trials. Simulation results are shown in Figure 8. The top figures show qualitatively the same results as obtained in (Mazzoni and Krakauer, 2006). The bottom figure shows the response of the internal models - both are estimating $-d(k) = 45$ (the minus sign is an artifact of our choice of parameters, and is

not significant). The second internal model is faster because it experiences more frequent updates.

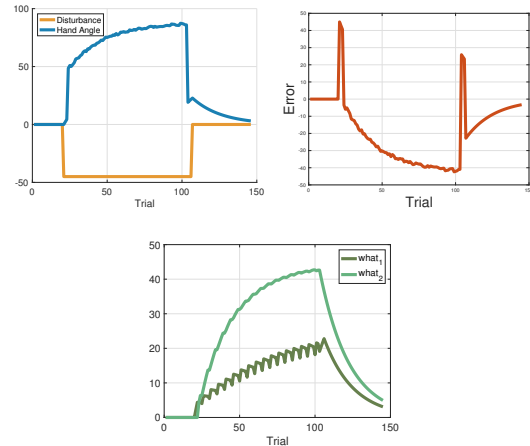


Figure 8: Mazzoni and Krakauer’s experiment. The top left figure displays the disturbance $d(k)$ and the hand angle $x(k)$ as a function of the trial number k . The top right figure shows the error $e(k)$ with respect to the first target only. The bottom figure shows the internal model states $\hat{w}_1(k)$, $\hat{w}_2(k)$ as a function of k .

8 CONCLUSION

This paper has presented an overview of results on the use of regulator theory to interpret and model the contribution of the cerebellum to motor systems. We considered the slow eye movement systems: the VOR, gaze holding, and smooth pursuit, as well as the optokinetic system. We found that using regulator theory one could derive models that are consistent with the known neural circuits and also recover the standard experimental results for those motor systems. We also surveyed results for visuomotor adaptation; despite the fact that the models are discrete-time difference equations rather than differential equations, a nearly identical methodology as in continuous time could be employed to derive a model that recovers many of the standard experimental results.

The paper has several takeaways on the form of the resulting internal models, and what they may tell us about the cerebellum. A recurring pattern in the motor systems we examined is that the cerebellum must be endowed with a special capability to enable and disable internal models without causing damage to the body. We have identified the nucleo-cortical pathway as a possible mechanism to implement this capability.

Finally, this paper has argued that an approach to modeling the cerebellum based on regulator theory can well serve a research agenda to develop humanoid robots that possess cerebellar-like intelligences.

REFERENCES

- Apps, R., Hawkes, R., and et. al., S. A. (2018). Cerebellar modules and their role as operational cerebellar processing units. *Cerebellum*, 17:654–682.
- Barnes, G., Goodbody, S., and Collins, S. (1995). Volitional control of anticipatory ocular pursuit responses under stabilized image conditions in humans. *Experimental Brain Research*, 106:301–317.
- Battle, E. and Broucke, M. (2021). Adaptive internal models in the optokinetic system. In *IEEE Conference on Decision and Control*. Submitted.
- Bond, K. and Taylor, J. (2015). Flexible explicit but rigid implicit learning in a visuomotor adaptation task. *Journal of Neurophysiology*, 113:3836–3849.
- Broucke, M. E. (2020). Model of the oculomotor system based on adaptive internal models. *IFAC-PapersOnLine*, 53(2):16430–16437. 21th IFAC World Congress.
- Broucke, M. E. (2021). Adaptive internal model theory of the oculomotor system and the cerebellum. *IEEE Transactions on Automatic Control*.
- Büttner, U. and Büttner-Ennever, J. (2006). Present concepts of oculomotor organization. *Prog. Brain Research*, 151:1–42.
- Büttner, U., Waespe, W., and Henn, V. (1976). Duration and direction of optokinetic after-nystagmus as a function of stimulus exposure time in the monkey. *Arch. Psychiat. Nervenkr.*, 222:281–291.
- Cominola, N., Apps, R., and Marple-Horvat, D. (2009). An internal model of a moving visual target in the lateral cerebellum. *J. Physiology*, 587(2):429–442.
- Churchland, M., Chou, I., and Lisberger, S. (2003). Evidence for object permanence in the smooth-pursuit eye movements of monkeys. *Journal of Neurophysiology*, 90:2205–2218.
- Cohen, B., Matsuo, V., and Raphan, T. (1977). Quantitative analysis of the velocity characteristics of optokinetic nystagmus and optokinetic after-nystagmus. *J. Physiology*, 270:321–344.
- de Brouwer, A., Albaghdadi, M., Flanagan, J., and Gallivan, J. (2018). Using gaze behavior to parcellate the explicit and implicit contributions to visuomotor learning. *Journal of Neurophysiology*, 120:1602–1615.
- Eccles, J., Ito, M., and Szentagothai, J. (1967). *The Cerebellum as a Neuronal Machine*. Springer.
- Francis, B. and Wonham, W. (1976). The internal model principle of control theory. *Automatica*, 12:457–465.
- Fujita, M. (1982). Adaptive filter model of the cerebellum. *Biological Cybernetics*, 45:195–206.
- Galea, J., Vazquez, A., Pasricha, N., de Xivry, J., and Celnik, P. (2011). Dissociating the roles of the cerebellum and motor cortex during adaptive learning: the motor cortex retains what the cerebellum learns. *Cerebral Cortex*, 21:1761–1770.
- Gawad, A. A. and Broucke, M. E. (2020). Visuomotor adaptation is a disturbance rejection problem. In *IEEE Conference on Decision and Control*, pages 3895–3900.
- Hafez, M., Uzeda, E., and Broucke, M. (2021). Discrete-time output regulation and visuomotor adaptation. *Letters of the Control Systems Society*. Submitted.
- Houck, B. D. and Person, A. L. (2014). Cerebellar loops: a review of the nucleocortical pathway. *Cerebellum*, 13:378–385.
- Ito, M. (1984). *The Cerebellum and Neural Control*. Raven Press.
- Kanellakopoulos, M. K. I. and Kokotovic, P. (1995). *Nonlinear and Adaptive Control Design*. Wiley-Interscience.
- Kitago, T., Ryan, S., Mazzoni, P., Krakauer, J., and Haith, A. (2013). Unlearning versus savings in visuomotor adaptation: comparing effects of washout, passage of time, and removal of errors on motor memory. *Frontiers in Human Neuroscience*, 7(307).
- Kojima, Y., Iwamoto, Y., and Yoshida, K. (2004). Memory of learning facilitates saccadic adaptation in the monkey. *Journal of Neuroscience*, 24(34):7531–7539.
- Kreisselmeier, G. (1977). Adaptive observers with exponential rate of convergence. *IEEE Transactions on Automatic Control*, 22(1):2–8.
- Leigh, R. J. and Zee, D. S. (2015). *The Neurology of Eye Movements*. Oxford University Press, 5th ed.
- Lisberger, S. (2009). Internal models of eye movement in the floccular complex of the monkey cerebellum. *Neuroscience*, 162(3):763–776.
- Martin, T., Keating, J., Goodkin, H., Bastian, A., and Thach, W. (1996). Throwing while looking through prisms ii. specificity and storage of multiple gaze-throw calibrations. *Brain*, 119:1199 – 1211.
- Mazzoni, P. and Krakauer, J. (2006). An implicit plan overrides an explicit strategy during visuomotor adaptation. *Journal of Neuroscience*, 26:3642–3645.
- Miki, S., Urase, K., Baker, R., and Hirata, Y. (2020). Velocity storage mechanism drives a cerebellar clock for predictive eye velocity control. *Nature Science Reports*, 10(6944).
- Morris, E. and Lisberger, S. (1987). Different responses to small visual errors during initiation and maintenance of smooth-pursuit eye movements in monkeys. *Journal of Neurophysiology*, 58(6):1351–1369.
- Narendra, K. and Annaswamy, A. (1989). *Stable Adaptive Systems*. Dover Publications.
- Nikiforov, V. O. (2004a). Observers of external deterministic disturbances i. objects with known parameters. *Automation and Remote Control*, 65(10):1531–1541.
- Nikiforov, V. O. (2004b). Observers of external deterministic disturbances ii. objects with unknown parameters. *Automation and Remote Control*, 65(11):1724–1732.
- Ramachandran, R. and Lisberger, S. (2008). Neural substrate of modified and unmodified pathways for learning in monkey vestibuloocular reflex. *J. Neurophysiology*, 100:1868–1878.
- Rand, M. and Rentsch, S. (2015). Gaze locations affect explicit process but not implicit process during visuomotor adaptation. *Journal of Neurophysiology*, 113:88–99.

- Raphan, T., Matsuo, V., and Cohen, B. (1979). Velocity storage in the vestibulo-ocular reflex arc (vor). *Experimental Brain Research*, 35:229–248.
- Robinson, D. A. (1974). The effect of cerebellectomy on the cat's vestibulo-ocular integrator. *Brain Research*, 71(2):195–207.
- Ruigrok, T. (2011). Ins and outs of cerebellar modules. *Cerebellum*, 10:464–474.
- Saberi, A., Stoorvogel, A., and Sannuti, P. (2000). *Control of Linear Systems with Regulation and Input Constraints*. Springer.
- Serrani, A. and Isidori, A. (2000). Semiglobal nonlinear output regulation with adaptive internal model. *IEEE Conference on Decision and Control*, pages 1649–1654.
- Serrani, A., Isidori, A., and Marconi, L. (2001). Semiglobal nonlinear output regulation with adaptive internal model. *IEEE Transactions on Automatic Control*, 46(8):1178–1194.
- Shadmehr, R. and Wise, S. (2005). *The Computational Neurobiology of Reaching and Pointing*. MIT Press.
- Shmuelof, L., Hang, V., Haith, A., Dekicki, R., Mazzoni, P., and Krakauer, J. (2012). Overcoming motor forgetting through reinforcement of learned actions. *Journal of Neuroscience*, 32(42):14617–14621.
- Smith, M., Ghazizadeh, A., and Shadmehr, R. (2006). Interacting adaptive processes with different timescales underlie short-term motor learning. *PLOS Computational Biology*, 4(6).
- Stone, L. S. and Lisberger, S. G. (1990). Visual responses of purkinje cells in the cerebellar flocculus during smooth-pursuit eye movements in monkeys. i. simple spikes. *Journal of Neurophysiology*, 63(5):1241–1261.
- Sylvestre, P. A. and Cullen, K. E. (1999). Quantitative analysis of abducens neuron discharge dynamics during saccadic and slow eye movements. *Journal of Neurophysiology*, 82(5):2612–2632.
- Vaswani, P., Shmuelof, L., Haith, A., Deknicki, R., Huang, V., Mazzoni, P., Shadmehr, R., and Krakauer, J. (2015). Persistent residual errors in motor adaptation tasks: reversion to baseline and exploratory escape. *Journal of Neuroscience*, 35(17):6969–6977.
- Waespe, W. and Henn, V. (1978a). Conflicting visual-vestibular stimulation and vestibular nucleus activity in alert monkeys. *Experimental Brain Research*, 33:203–211.
- Waespe, W. and Henn, V. (1978b). Reciprocal changes in primary and secondary optokinetic after-nystagmus (okan) produced by repetitive optokinetic stimulation in the monkey. *Archiv Psychiatrie und Nervenkrankheiten*, 225:23–30.
- Wonham, W. M. (1985). *Linear Multivariable Control: a Geometric Approach*. Springer-Verlag.